

Intelligent Biomimetic Artificial Form for Lignocellulosic Surfaces

Doğru RAMAZANOĞLU^{1*}  Ferhat ÖZDEMİR¹ 

¹Kahramanmaraş Sütçü İmam University, Forest Industry Engineering, Kahramanmaraş, TURKEY

*Corresponding Author: doguramazoglu@hotmail.com

Received Date: 04.04.2020

Accepted Date: 17.03.2021

Abstract

Aim of study: In this study, it is aimed to make the wood material hydrophobic and magnetic by creating a smart biomimetic artificial form for lignocellulosic surfaces.

Material and methods: Ferrous sulfate heptahydrate ($\text{FeSO}_4 \cdot 7\text{H}_2\text{O}$), Manganese (II) chloride ($\text{MnCl}_2 \cdot 4\text{H}_2\text{O}$), Ethyl alcohol (EtOH), Sodium hydroxide (NaOH), and Potassium nitrate (KNO_3) having implemented on the wood to the synthesis of the intelligent biomimetic surface. Hydrophobisation had supplied by Octadecyltrichlorosilane (OTS, 95%). Fourier-transform infrared spectroscopy (FTIR), X-ray diffraction (XRD), Scanning electron microscopy (SEM), and Energy dispersive x-ray (EDX) having used for the characterization step. Water contact angle (WCA) had used for hydrophobicity. Finally, the UV-Vis spectrometer device had used to determine the magnetic properties.

Main results: According to the characterizations, the smart biomimetic artificial form having been synthesized on a wood surface successfully. The water contact angle of the new surface having determined as $\theta \approx 125^\circ$. It showed absorption properties in the wavelength range of 200-800 nm.

Highlights: As a smart biomimetic artificial design has produced as a result of this study improves the resistance of wood to water and sunshine, this could be significantly diminished maintenance costs in many fields from living areas to the maritime industry.

Keywords: Intelligent, Biomimetic, Artificial Surface Form

Lignoselülozik Yüzeyler için Akıllı Biyomimetik Yapay Form

Öz

Çalışmanın amacı: Bu çalışmada, lignoselülozik yüzeyler için akıllı biyomimetik yapay form oluşturup ahşap malzemenin hidrofobik ve manyetik özellik kazanması amaçlanmıştır.

Materyal ve yöntem: Akıllı biyomimetik yapay yüzeyin oluşturulması için Demirli sülfat heptahidrat ($\text{FeSO}_4 \cdot 7\text{H}_2\text{O}$), Manganez (II) klorür ($\text{MnCl}_2 \cdot 4\text{H}_2\text{O}$), Etil alkol (EtOH), Sodyum hidroksit (NaOH) ve Potasyum nitrat (KNO_3) kullanılarak masif yüzeye hidrotermal olarak uygulanmıştır. Hidrofobizasyon Oktadesiltri-klorosilan (OTS, %95) kullanılarak sağlanmıştır. Modifikasyon çalışmalarını karakterize etmek için Fourier dönüşümü kızılötesi spektroskopisi (FTIR), X-ışını kırınımı (XRD), Taramalı elektron Mikroskopisi (SEM) ve Enerji dağıtıcı x-ışını (EDX) analizleri yapılmıştır. Hidrofobiklik özelliğinin belirlenmesi için su temas açısı (WCA) ve son olarak manyetik özelliklerini belirlemek için UV-Vis spektrometre cihazı kullanılmıştır.

Temel sonuçlar: Yapılan karakterizasyon çalışmaları ahşap yüzeyde akıllı biyomimetik yapay form başarılı bir şekilde oluşturulduğunu göstermektedir. Yeni yüzeyin su temas açısı $\theta \approx 125^\circ$ olarak belirlenmiştir. 200-800 nm dalga boyu aralığında absorpsiyon özellik göstermiştir.

Araştırma vurguları: Bu çalışma sonucunda üretilen akıllı biyomimetik yapay form ahşabın suya ve güneş ışığına olan dayanımını artırdığı için yaşam alanlarından denizcilik sektörüne kadar birçok alandaki bakım maliyetlerini önemli ölçüde azaltabilir.

Anahtar Kelimeler: Akıllı, Biyomimetik, Yapay Yüzey Formu



Introduction

The idea of functionalizing the wooden surface with nanomagnetic particles having been proposed by (Oka & Fujita, 1999) firstly. Thus, it had intended to reduce the damage-causing by electromagnetic wave absorbers in indoor spaces. UV rays on outdoor surfaces in outdoor spaces (Oka & Fujita, 1999; Oka et al., 2002a; Oka et al., 2002b; Oka et al., 2004a; Oka et al., 2004b; Oka et al., 2007; Oka et al., 2011).

However, the formation of excess hydrophilic structure in the final product increased UV degeneration while decreasing water and moisture resistance.

It is inevitable that wood materials have been using in the outdoor environment will be exposed to UV rays as well as other environmental factors such as water and moisture. On the other hand, it would not be wrong to say that the effect of UV rays on the wood structure are more than the damage caused by water and moisture. Lignin suffers the most from the UV radiation to which the wood surface exposed. As a result of this UV radiation, lignin breaks down, causing many radical groups to form. When these radicals come into contact with oxygen in the air, color changes had observed on the surface of the wood (Jirus-Rajkovic et al., 2004; Özdemir et al., 2018; Patachia et al., 2012; Ramazanoğlu & Özdemir, 2021; Salla et al., 2012).

Besides, it affects the wood structure negatively in other environmental factors such as temperature difference and humidity (Hayoz et al., 2003).

The porous and hydrophilic nature of the wood allows water to enter the lower layers. In addition, the expansion of water with temperature change causes cracking and breakage in woody structure. At the same time, this negative effect of water increases the damage of UV radiation to woody structure (Eichhorn et al., 2010; Hakkou et al., 2005; Lu et al., 2014). Therefore, surface treatment combined with hydrophobicity and magnetic properties was essential for the protection of wood-based materials. In the study, magnetic wood having obtained by positioning MnFe_2O_4 nanoparticles on the wood surface. Thus, a magnetic surface had received. Then, the magnetic property having

gained, the hydrophobicity of the surface has been supplied by OTS. Fourier-transform infrared spectroscopy, X-ray Diffraction, Scanning Electron Microscopy, and Energy Dispersive X-ray having conducted to the characterization of modification studies. The water contact angle having studied for the determination of surface hydrophobicity and UV-vis spectrometer device had been used for determination of magnetic properties.

Materials and Methods

Material

Beechwood species had purchased from a commercial market in Kahramanmaraş in Turkey. Ferrous sulfate heptahydrate ($\text{FeSO}_4 \cdot 7\text{H}_2\text{O}$) and Manganese (II) chloride ($\text{MnCl}_2 \cdot 4\text{H}_2\text{O}$) had supplied from Carlo Erba Reagents in Barcelona, Spain. Ethyl alcohol (EtOH) and Sodium hydroxide (NaOH) have been provided from TEKKİM in Istanbul, Turkey. Potassium nitrate (KNO_3) was bought from Darmstadt in Germany. Octadecyltrichlorosilane (OTS, 95%) was purchased from J.K.Chemicals, in Telangana, India.

Method

Thermogravimetric analyses were performed by EXSTAR TG/DTA 6300. SEM images and EDX spectra had ingested by Zeiss Eva 50 ED, and XRD spectra has taken via to Rigaku Rint 2000 brand device in KSÜ/ÜSKİM. Water contact angle measurements having been done by KSV Cam101 Scientific Instrument (Helsinki, Finland) brand devices located in the forest faculty of Istanbul University where been used.

The chemical route has developed for the synthesis of hydrophobic and magnetic wood has been given in Figure 1. Beechwood species cut into 2 mm (radial) x 10 mm (tangent) x 15 mm x (longitudinal) had been exposed to an ultrasonic bath for 30 minutes and had dried at 103 ± 2 °C for 48 h (step a). After, the ultrasonic bath, wood particles having added to an orange color reaction solution where the iron and manganese molar concentration ratio had adjusted as 2 ($[\text{Fe}^{2+}]/[\text{Mn}^{2+}] = 2$). The reactor has subjected to a 90 °C hydrothermal method for 3 hours.

The hydrothermal process was continued at 90°C for 6 hours with a new reaction solution prepared with 15 ml of 1.32 M sodium hydroxide (NaOH) and potassium nitrate solution (KNO₃) ($[\text{Fe}^{2+}]/[\text{NO}_3^-] = 0.44$). Thus, ferrite nanoparticles were coated on the wood surface to give high surface roughness and magnetic properties (step b). Finally, samples were washed in the ultrasonic bath for 30 minutes to remove unreacted chemical residues and dried in an oven at 50°C for 24 hours. Subsequently, 20

ml of 5% (V/V) Octadecyltrichlorosilane (OTS) was taken into ethanol solution and mixed for 24 hours at room temperature with a mechanical mixer and the magnetic surface of wood samples has covered by OTS molecules (step c). Finally, they have dried at 50°C for 24 hours. Thus, the hydrophobic wood surface had occurred (step d). Finally, they had dried at 50°C for 24 hours. Thus, the hydrophobic wood surface having obtained (step d).

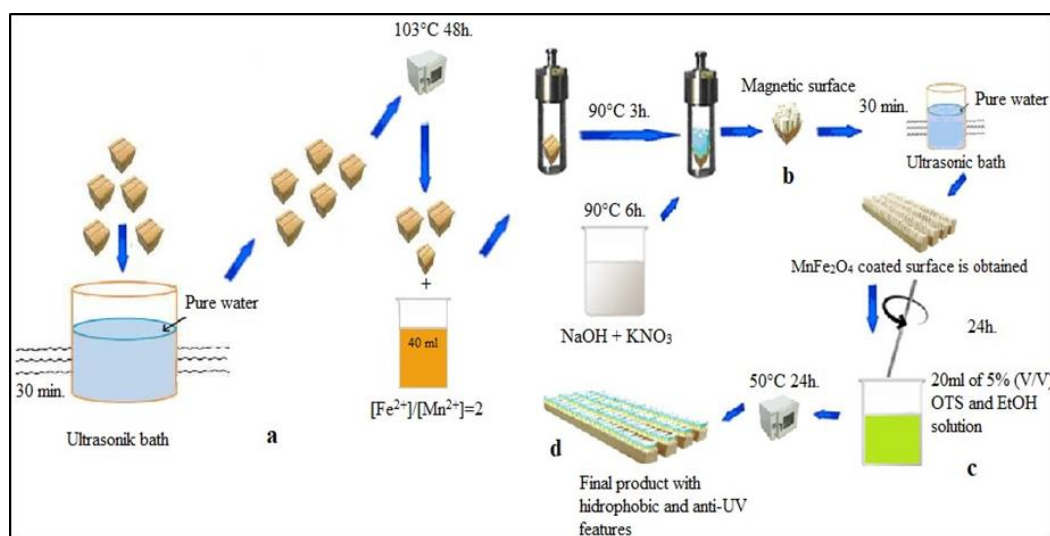


Figure 1. Schematic representation of the synthesis

Results and Discussion

Fourier-Transform Infrared Spectroscopy (FTIR)

The FTIR spectra of untreated wood, MnFe₂O₄ functional magnetic surface, and OTS functional samples had presented in Figure 2. It contains all the characteristic bands of massive wood as a control sample (Fig. 2a). It refers to the ~OH hydroxyl groups of cellulose in the broadband wood structure was detected at 3467 cm⁻¹ (Liang & Marchessault, 1959; Ramazanoğlu & Özdemir 2020; Ramazanoğlu & Özdemir 2021; Schwanninger et al., 2004).

In the massive spectrum, the peaks at 1735 cm⁻¹ and 1510 cm⁻¹ have been classified as ~C=O and ~C=C vibration in the cellulose

structure. Asymmetric peaks around 1422 cm⁻¹ indicate the ~C-H deformation in the methyl ~CH₃ groups in the cellulose structure (Lu et al., 2014). The narrowing in the wide ~OH band on the magnetic wood surface (Fig. 2b) is an indication of the positioning of the MnFe₂O₄ particles to the wood surface (Lu et al., 2014). It is Fe-O vibration on the peak surface at 632 cm⁻¹ on the magnetic surface (Waldron, 1955). C-H tensions in the methyl and methylene groups appear to be 2960 cm⁻¹ and belong to the methyl and ethylene groups (Faux, 1991). On the OTS coated surface, ~2825 cm⁻¹, ~2923 cm⁻¹ ~C-H tensions, and the Si-O-C peak at 1193 cm⁻¹ (Figure 2c) shows that OTS is attached to the lignocellulosic surface successfully.

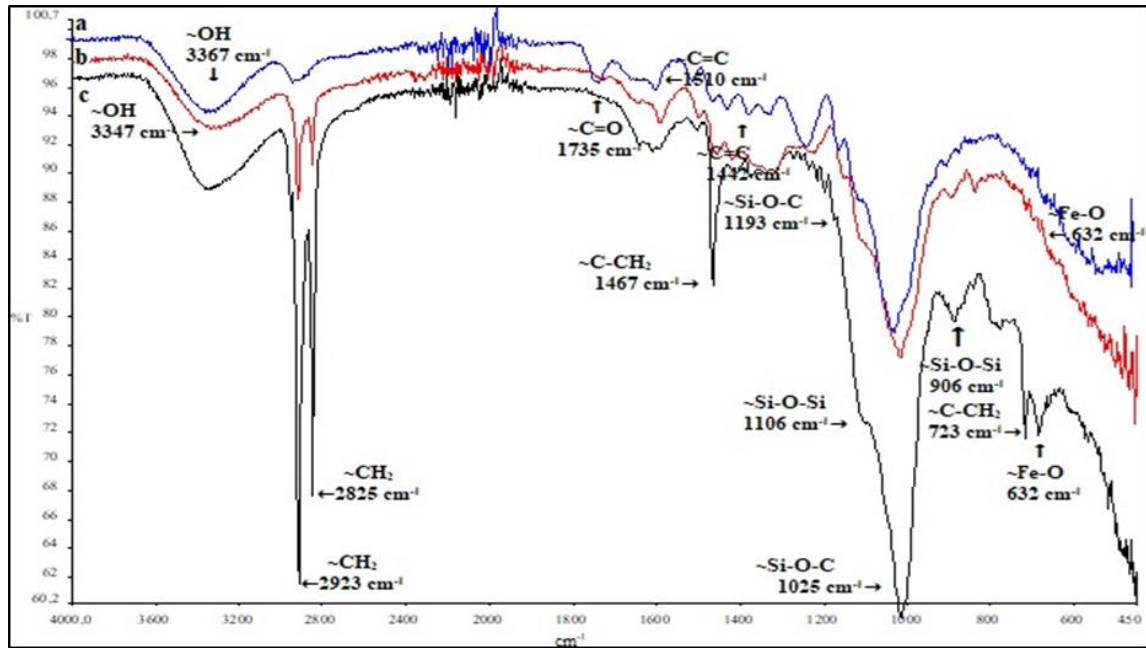


Figure 2. FTIR spectrum of (a) the untreated wood (b) magnetic wood and (c) OTS hydrolyzed

X-ray Diffraction (XRD)

The XRD spectra of the exposed samples to the hydrothermal process that molar concentration of iron and manganese had been fixed as $[Fe^{2+}]/[Mn^{2+}] = 2$ given in Figure 3. The peaks at 16.4° and 22.5° in (Figure 3a.) diffraction peaks indicate the characteristic

wood structure of the cellulose molecule (Andersson et al., 2003; Borysiak & Doczekalska, 2005; Kumar et al, 1993). Wood surface subjected to reactor solution prepared using 0.2 M. $FeSO_4 \cdot 7H_2O$ and $MnCl_2 \cdot 4H_2O$ stock solutions for 3 hours at $90^\circ C$.

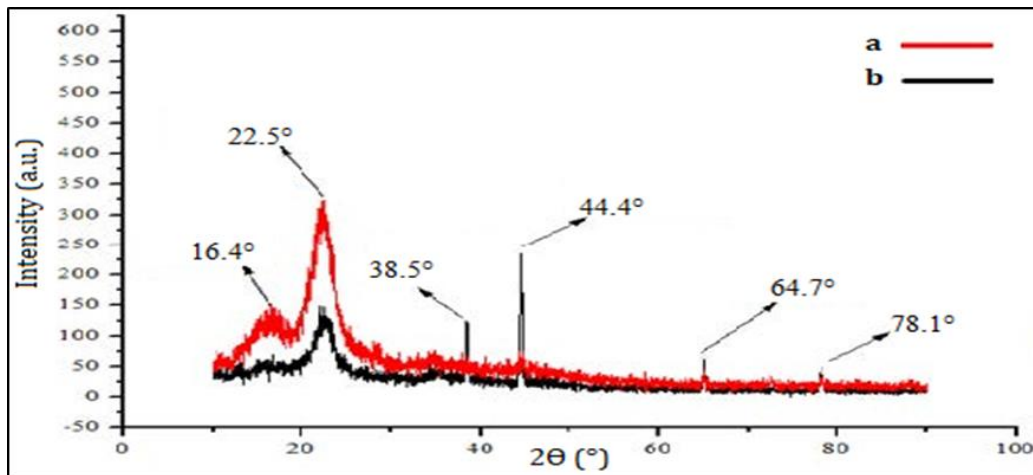


Figure 3. XRD spectra of (a) untreated wood, (b) magnetic wood which were functionalized with $MnFe_2O_4$ nanoparticles.

Scanning Electron Microscopy (SEM) & Energy Dispersive X-Ray (EDX)

SEM image and EDX spectra of the original wood sample, the wood sample coated with MnFe_2SO_4 nanoparticles, and hydrophobized wood surface have seen in (Figure 4).

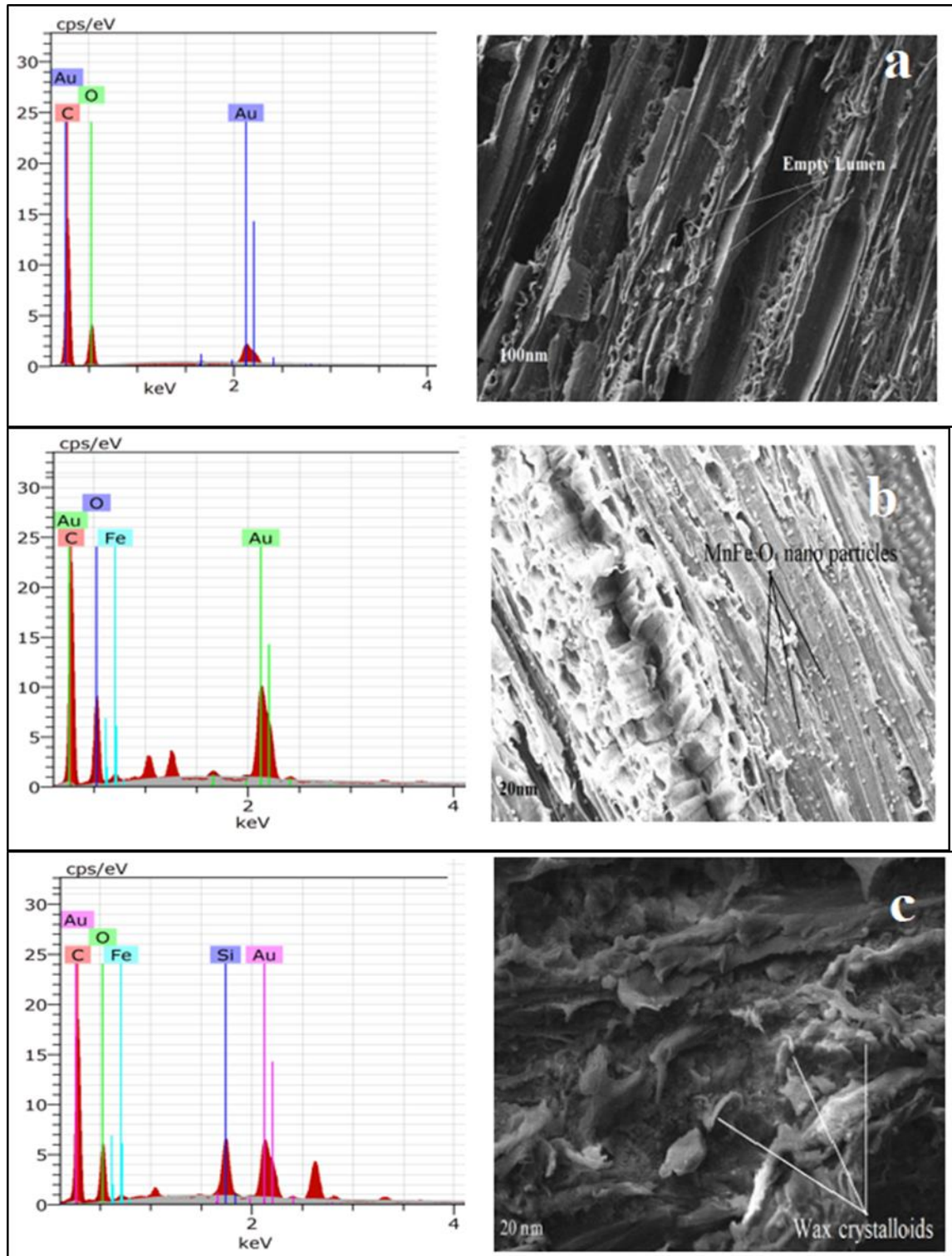


Figure 4. SEM image and EDX spectra, (a) untreated wood; (b) the wood sample treated with MnFe_2O_4 nano particles; (c) the wood sample treated with MnFe_2O_4 nano particles and OTS.

In the EDX spectrum of the massive sample (Figure 4a), the golden peak having seen due to the coating that provides surface conductivity with oxygen and carbon, which are individual peaks of the lignocellulosic structure.

In the EDX spectrum, the surface covered with MnFe_2SO_4 nanoparticles, it had observed that the iron (Fe) peak on the wooden surface was embraced by MnFe_2O_4 nanoparticles effectively in Figure 4b. In hydrophobization (Figure 4c.) the presence of the silane (Si) peak belonging to OTS has been determined (Gao et al., 2015a). In addition, in SEM images in Figure 4c, MnFe_2O_4 nanoscale protrusions and the thin layer was formed by wax crystalloids of OTS coated the wooden surface. The design of this type of binary structure essential for surface hydrophobization (Li et al., 2013; Lu et al., 2014; Ramazanoğlu & Özdemir, 2021; Xia et al., 2012).

Water Contact Angle (WCA)

Original wood sample (a), subjected to hydrothermal process with the reactor solution (b), only OTS-treated wood sample (c), and d) the wood samples with MnFe_2O_4 nanoparticles its surface treated by OTS under laboratory condition and their contact angles were given in (figure 5). While the water contact angle of the original wood has appeared as $\theta\gamma$ 84.7° (Figure 5a), the lower hydrophilicity due to the MnFe_2O_4 particles to be positioned on the lignocellulosic surface, causing the new water contact angle to has been measured as $\theta\gamma$ 34.6° (Figure 5b).

In a previous study, the value of WCA had measured as $\theta\gamma$ 100° as a result of the application of OTS directly on the massive (Gan et al., 2015). In this study, wood has hydrophobized directly with OTS. the water contact angle had increased about 23.9% and having measured $\theta\gamma$ 105° (Figure 5c). The hydrophilic surface had obtained as a result of adhering MnFe_2O_4 nanoparticles hydrophobicity had increased like 261% after the intervention with OTS with the value of $\theta\gamma$ 125° (Figure 5d)

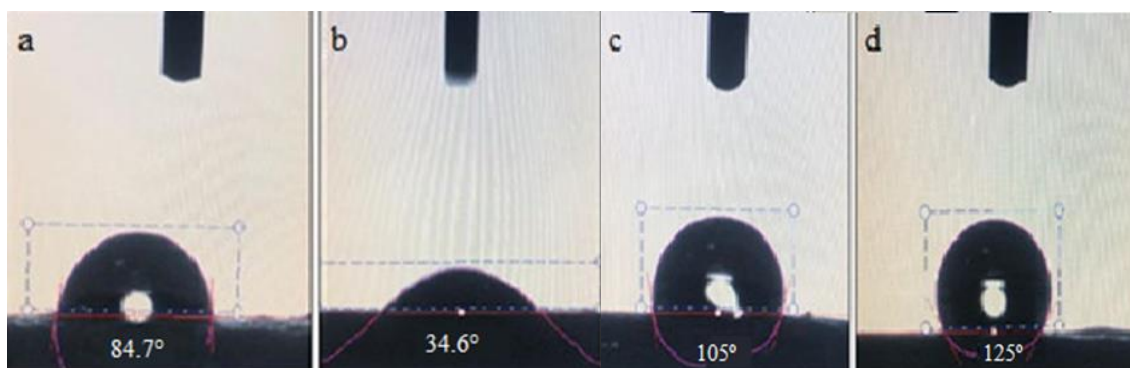


Figure 5. Water contact angle of (a) massive wood, (b) the wood treated by MnFe_2O_4 nanoparticles, (c) the wood treated by only OTS, and (d) the wood sample treated with MnFe_2O_4 nanoparticles and OTS

Ultraviolet and Visible Light (UV-Vis)

The UV spectra of the solid wood and the magnetic wood had obtained by hydrothermal functioning of the surface with MnFe_2O_4 nanoparticles were given in Figure 6. The solid wood and the magnetic wood had obtained by hydrothermal functioning of the surface with MnFe_2O_4 nanoparticles were presented in Figure 6. (Zhu et al. 2011) stated that the magnetic wood obtained by CoFe_2O_4 nanoparticles in 2011 show absorption

properties between 200-800 nm wavelength (Zhu et al., 2011). The magnetic wood had been formed via MnFe_2O_4 nanoparticles instead of cobalt and compared at 200-800 nm wavelength. Thanks to the magnetic feature (Ramazanoğlu & Özdemir, 2020; Ramazanoğlu & Özdemir 2021) via functionalized MnFe_2O_4 nanoparticles, wavelength UV lights were not absorbed well by the MnFe_2O_4 nanoparticles. But, the sunshine range about 400-800 nm has

wavelength exhibits a much higher absorption than untreated wood. Thus, photodegradation was not able to perform on woody components (Donath et al., 2007; Ramazanoğlu, 2020). Magnetic wood coated with MnFe_2O_4 nanoparticles showed the highest absorption performance between 400-800 nm wavelength.

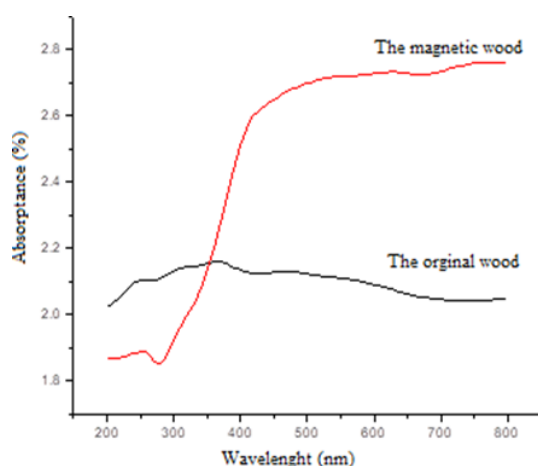


Figure 6. UV spectrum of the original wood; untreated massive wood sample, and the magnetic wood; magnetic wood coated with MnFe_2O_4 nanoparticles

Conclusion

Wood is the most reliable material from the existence of the earth to the present day. Human beings have used wood for different purposes in many fields. The study aimed that reducing the sensitivity of wood for moisture and sunlight due to its lignocellulosic nature. In line with this aim;

Using the low-temperature hydrothermal method help to MnFe_2O_4 nanoparticles were positioned on the wooden surface; Thus, photodegradation caused by sun rays having prevented thanks to its magnetic feature.

The wood has been gained magnetic properties with MnFe_2O_4 particles at the low-temperature hydrothermal method. Then, the hydrophobic property affixed to this magnetic surface mixed with OTS at room temperature mechanically.

At the characterization, the narrowing wide $\sim\text{OH}$ band evidence that MnFe_2O_4 particles having located on the lignocellulosic surface in the FTIR spectrum. The peaks having performed about $\sim 2825\text{ cm}^{-1}$, $\sim 2923\text{ cm}^{-1}$ from $\sim\text{C-H}$ tensions, and the Si-O-C

peak has resembled at 1193 cm^{-1} exhibits that OTS bounded to MnFe_2O_4 treated wood successfully too. In the XRD spectrum; The peaks appeared at 16.8° , 22.0° , 38.5° , 44.4° , 67.7° , and 78.1° indicate that the MnFe_2O_4 nanoparticles were attached to the lignocellulosic surface.

SEM images and the EDX spectrum also prove that MnFe_2O_4 nanoparticles having located on a wood surface with a Fe peak (Fig. 4b). Additionally, the presence of the silane (Si) peak belonging to OTS (Fig. 4b.) shows hydrophobization completed. In WCA, there was a lessening from $\theta\gamma 84.7^\circ$ to $\theta\gamma 34.6^\circ$ those shows, MnFe_2O_4 nanoparticles modification having accomplished. Moreover, the rise in WCAs from $\theta\gamma 34.6^\circ$ to $\theta\gamma 125^\circ$ shows that magnetic surface having coating by OTS successfully.

In the UV-vis spectrometer, the surface coated with MnFe_2O_4 nanoparticles has much higher UV absorption than untreated wood. It means that MnFe_2O_4 nanoparticles were located on the wood surface and supplied magnetic feature.

Consequently, the wood having gained self-protection from sun rays and self-cleaning features by this synthesized multifunctional wood surface.

Acknowledgements

The authors are grateful for supporting this project by the Scientific Research Projects Coordination Department of Kahramanmaraş Sutcu Imam University.

Ethics Committee Approval

N/A

Peer-review

Externally peer-reviewed.

Author Contributions

Conceptualization: D.R., F.Ö.; Investigation: D.R.; Material and Methodology: D.R., F.Ö.; Supervision: F.Ö.; Visualization: D.R.; Writing-Original Draft: D.R.; Writing-review & Editing: D.R.; Other: All authors have read and agreed to the published version of manuscript.

Conflict of Interest

The authors have no conflicts of interest to declare.

Funding

This study has been supported within the scope of project numbered 2018/3-20 D. by Kahramanmaraş Sutcu Imam University, Scientific Research Projects Coordination Department.

References

- Andersson, S., Serimaa, R., Paakkari, T., Saranpaää, P. & Pesonen, E. (2003). Crystallinity of wood and the size of cellulose crystallites in Norway spruce (*Picea abies*). *Journal of Wood Science*, 49, 531 -537.
- Borysiak, S. & Doczekalska, B. (2005). X-ray Diffraction study of pine wood treated with NaOH fibers. *Textiles Eastern Europe*, 13, 87-89.
- Donath, S., Militz, H. & Mai, C. (2007). Weathering of silane treated wood, *Holz. Roh. Werkst.* 65, 35-42.
- Eichhorn, S. J., Dufresne, A. & Aranguren, M. (2010). Review: current international research into cellulose nanofibers and nanocomposites. *Journal of Materials Science*, 45, 1-33.
- Faux, O. (1991). Classification of Lignins from different botanical origins by FT-IR spectroscopy. *Holzforschung*, 45, 21-28.
- Gao, L., Lu, Y., Zhan, X. & Sun, Q. (2015a). A robust, anti-acid, and high-temperature humidity-resistant superhydrophobic surface of wood based on a modified TiO₂ film by fluoroalkyl silane. *Surface and Coatings Technology*, 262, 33-39.
- Gan, W. T., Gao, L. K., Sun, F. Q., Jin, C. D., Lu, Y. & Li, J. (2015). Multifunctional wood materials with magnetic, superhydrophobic and anti-ultraviolet properties. *Applied Surface Science*, 322, 565-572.
- Hakkou, M., Pétrissans, M. & Zoulalian, A. (2005). Investigation of wood wettability changes during heat treatment on the basis of chemical analysis. *Polymer Degradation Stability Journal*, 89, 1-5.
- Hayoz, P., Peter, W. & Rogez, D. (2003). A new innovative stabilization method for the protection of natural wood. *Prog. Org. Coat*, 48, 297-309.
- Jirous-Rajkovic, V., Bogner, A. & Radovan, D. (2004). The efficiency of various treatments in protecting wood surfaces against weathering. *Surface and Coatings Technology*, 87, 15-19.
- Kumar, M., Gupta, R. C. & Sharma, T. (1993). X-ray diffraction studies of acacia and eucalyptus wood chars. *Journal of Materials Science*. 28, 805.
- Li, N., Xia, T., Heng, L. & Liu, L. (2013). Superhydrophobic Zr-based metallic glass surface with high adhesive force. *Applied Physics Letters*, 102, 251603.
- Liang, C.Y. & Marchessault, R.H. (1959). Infrared Spectra of crystalline polysaccharides. hydrogen bonds in native celluloses. *Journal of Polymer Science*, 37, 385-395.
- Lu, Y., Xiao, S., Gao, R., Li, J. & Sun, Q. (2014). Improved weathering performance and wettability of wood protected by CeO₂ coating deposited onto the surface, *Holzforschung*, 68, 345-351.
- Oka, H., Kataoka, Y., Osada, H. & Aruga, Y. (2007). Experimental study on electromagnetic wave absorbing control of coating-type magnetic wood using a grooving process. *Journal of Magnetism and Magnetic Materials*, 310, E1028-E1029.
- Oka, H., Hamano, H. & Chiba, S. (2004a). Experimental study on actuation functions of coating-type magnetic. *Journal of Magnetism and Magnetic Materials*, 272, E1693-E1694.
- Oka, H., Hojo, A., Seki, K. & Takashiba, T. (2002a). Wood construction and magnetic characteristics of impregnated type magnetic wood. *Journal of Magnetism and Magnetic Materials*, 239, 617-619.
- Oka, H., Narita, K., Osada, H. & Seki, K. (2002b). Experimental results on indoor electromagnetic wave absorber using magnetic wood. *Journal of Applied Physics*, 91, 7008-7010.
- Oka, H., Tokuta, H., Namizaki, Y. & Sekino, N. (2004b). Effects of humidity on the magnetic and woody characteristics of powder-type magnetic wood. *Journal of Magnetism and Magnetic Materials*, 272, 1515-1517.
- Oka, H., Uchidate, S. & Sekino, N. (2011). Electromagnetic wave absorption characteristics of half carbonized powder-type magnetic wood. *IEEE. Transactions on Magnetics*, 47, 3078-3080.
- Oka, H. & Fujita, H. (1999). Experimental study on magnetic and heating characteristics of magnetic wood. *Journal of Applied Physics*, 85(8), 5732-5734
- Özdemir, F., Ramazanoglu, D., Tutus, A. (2018). Investigation of the effect of aging time, sanding and section direction on surface quality of fir wood, *Journal of Bartın Faculty of Forestry*, vol. 20 (2): 194-204.
- Patachia, S., Croitoru, C. & Friedrich, C. (2012). Effect of uv exposure on the surface chemistry of wood veneers treated with ionic liquids. *Applied Surface Science*, 258, 6723-6729.

- Ramazanoğlu, D. (2020). Design of smart biomimetic nanohybrid surface forms and investigation of hydrothermal modification on the lignocellulosic surface (Ph.D. Dissertation, Kahramanmaraş Sutcu Imam University, Kahramanmaraş, Turkey).
- Ramazanoğlu, D. & Özdemir, F. (2020). Hidrotermal yaklaşımın lignoselülozik yüzeydeki akıllı nano biyomimetik yansıması. *Turkish Journal of Forestry*, 21(3), 324-331.
- Ramazanoğlu, D. & Özdemir, F. (2021). ZnO-based nano biomimetic smart artificial form located on lignocellulosic surface with hydrothermal approach. *Kastamonu University Journal of Forestry Faculty*, 21 (1), 12-20.
- Salla, J., Pandey, K. K. & Srinivas, K. (2012). Improvement of uv resistance of Wood surfaces by using ZnO nanoparticles. *Polymer Degradation Stability Journal*, 97, 592-596.
- Schwanninger, M., Rodrigues, J. C., Pereira, H. & Hinterstoisser, B. (2004). Effects of short-time vibratory ball milling on the shape of FT-IR spectra of wood and cellulose. *Vibrational Spectroscopy*, 36, 23-40.
- Waldron, R. D. 1955. Infrared spectra of ferrites. *Physical Review Journals*, American Physical Society, 99(6), 1727-1735.
- Xia, T., Li, N., Wu, Y. & Liu, L. (2012). Patterned superhydrophobic surface based on pd based metallic glass. *Applied Physics Letters*, 101, 081601.
- Zhu, Z., Li, X., Zhao, Q., Shi, Y., Li, H. & Chen, G. (2011). Surface photovoltage properties and photocatalytic activities of nanocrystalline CoFe₂O₄ particles with porous superstructure fabricated by a modified chemical coprecipitation method. *Journal of Nanoparticle Research*, 13, 2147-2155.